JOURNAL OF VIROLOGY, Dec. 2011, p. 13195–13203 Vol. 85, No. 24
0022-538X/11/$12.00 doi:10.1128/JVI.00859-11

Avian-Type Receptor-Binding Ability Can Increase Influenza Virus Pathogenicity in Macaques▽#

Tokiko Watanabe,[1,2]†* Kyoko Shinya,[3]† Shinji Watanabe,[1,2]† Masaki Imai,[1]† Masato Hatta,[1]† Chengjun Li,[1] Ben F. Wolter,[1,4,5] Gabriele Neumann,[1] Anthony Hanson,[1] Makoto Ozawa,[1] Shinya Yamada,[6] Hirotaka Imai,[6] Saori Sakabe,[6] Ryo Takano,[6] Kiyoko Iwatsuki-Horimoto,[6] Maki Kiso,[6] Mutsumi Ito,[6] Satoshi Fukuyama,[2] Eiryo Kawakami,[6] Takeo Gorai,[6] Heather A. Simmons,[4] Daniel Schenkman,[1,4] Kevin Brunner,[4] Saverio V. Capuano III,[4] Jason T. Weinfurter,[1,4,5] Wataru Nishio,[7] Yoshimasa Maniwa,[7] Tatsuhiko Igarashi,[8] Akiko Makino,[3] Emily A. Travanty,[9] Jieru Wang,[9] Anette Kilander,[10] Susanne G. Dudman,[10] M. Suresh,[1] Robert J. Mason,[9] Olav Hungnes,[10] Thomas C. Friedrich,[1,4,5] and Yoshihiro Kawaoka[1,2,3,6,11]*

Department of Pathobiological Sciences, University of Wisconsin-Madison, Madison, Wisconsin 53711[1]; ERATO Infection-Induced Host Responses Project, Saitama 332-0012, Japan[2]; Department of Microbiology and Infectious Diseases, Kobe University, Hyogo 650-0017, Japan[3]; Wisconsin National Primate Research Center, University of Wisconsin-Madison, Madison, Wisconsin 53715[4]; AIDS Vaccine Research Laboratory, University of Wisconsin-Madison, Madison, Wisconsin 53711[5]; Division of Virology, Department of Microbiology and Immunology, Institute of Medical Science, University of Tokyo, Tokyo 108-8639, Japan[6]; Department of Surgery, Division of Thoracic Surgery, Kobe University, Hyogo 650-0017, Japan[7]; Laboratory of Primate Model, Experimental Research Center for Infectious Diseases, Institute for Virus Research, Kyoto University, Sakyo-ku, Kyoto 606-8507, Japan[8]; Department of Medicine, National Jewish Health, Denver, Colorado 80206[9]; Department of Virology, Norwegian Institute of Public Health, P.O. Box 4404 Nydalen, N-0403 Oslo, Norway[10]; and Department of Special Pathogens, International Research Center for Infectious Diseases, Institute of Medical Science, University of Tokyo, Minato-ku, Tokyo 108-8639, Japan[11]

Received 28 April 2011/Accepted 11 September 2011

The first influenza pandemic of the 21st century was caused by novel H1N1 viruses that emerged in early 2009. An Asp-to-Gly change at position 222 of the receptor-binding protein hemagglutinin (HA) correlates with more-severe infections in humans. The amino acid at position 222 of HA contributes to receptor-binding specificity with Asp (typically found in human influenza viruses) and Gly (typically found in avian and classic H1N1 swine influenza viruses), conferring binding to human- and avian-type receptors, respectively. Here, we asked whether binding to avian-type receptors enhances influenza virus pathogenicity. We tested two 2009 pandemic H1N1 viruses possessing HA-222G (isolated from severe cases) and two viruses that possessed HA-222D. In glycan arrays, viruses possessing HA-222D preferentially bound to human-type receptors, while those encoding HA-222G bound to both avian- and human-type receptors. This difference in receptor binding correlated with efficient infection of viruses possessing HA-222G, compared to those possessing HA-222D, in human lung tissue, including alveolar type II pneumocytes, which express avian-type receptors. In a nonhuman primate model, infection with one of the viruses possessing HA-222G caused lung damage more severe than did infection with a virus encoding HA-222D, although these pathological differences were not observed for the other virus pair with either HA-222G or HA-222D. These data demonstrate that the acquisition of avian-type receptor-binding specificity may result in more-efficient infection of human alveolar type II pneumocytes and thus more-severe lung damage. Collectively, these findings suggest a new mechanism by which influenza viruses may become more pathogenic in mammals, including humans.

In the early spring of 2009, the human population was confronted by a novel swine origin H1N1 influenza virus that caused the first influenza pandemic of the 21st century. In most cases, human infections with this virus appeared to be mild; however, many severe and fatal cases were reported in individuals who had no other underlying health issues (3). Yet, the virulence factors of the 2009 pandemic H1N1 virus, if any, remain poorly understood.

Host range and pathogenicity of influenza viruses are determined by both viral and host factors. The receptor-binding specificity of the hemagglutinin (HA) protein plays a role in host range restriction (18). In general, human influenza viruses preferentially bind to sialic acid linked to galactose by an α2,6 linkage (SAα2,6Gal), which is prevalent in human airway epithelium, whereas avian influenza viruses have higher affinity for SAα2,3Gal, the major sialyloligosaccharide species in duck intestine, where aquatic bird influenza viruses replicate (24).

* Corresponding author. mailing address: Influenza Research Institute, University of Wisconsin-Madison, 575 Science Drive, Madison, WI 53711. Phone: (608) 265-4925. Fax: (608) 265-5622. E-mail for Tokiko Watanabe: twatanabe@svm.vetmed.wisc.edu. E-mail for Yoshihiro Kawaoka: kawaokay@svm.vetmed.wisc.edu.

† These authors contributed equally to this work.

Supplemental material for this article may be found at http://jvi.asm.org/.

▽ Published ahead of print on 21 September 2011.

Receptor-binding specificities are determined by specific amino acids in HA that characterize avian or human influenza viruses (17, 24). Typically, the HAs of avian H1 influenza viruses possess Glu and Gly at positions 187 and 222 (H1 numbering; positions 190 and 225 in H3 numbering), which confer preferential binding to SAα2,3Gal receptors, whereas the HAs of human H1 influenza viruses typically encode Asp at both of these positions, which confers preferential binding to SAα2,6Gal (17). Interestingly, for the 1918 pandemic influenza strains, there are two variants of the HA protein, with either Gly or Asp at position 222, that differ in their abilities to bind to avian-type receptors (28). However, it is not known if these differences in receptor specificity affected the pathogenicity of the 1918 pandemic virus in humans.

The 2009 pandemic H1N1 influenza viruses encode Asp at both positions, resembling seasonal human influenza viruses in this regard. Notably, some 2009 pandemic H1N1 influenza viruses possess Gly (i.e., the avian-type amino acid) at position 222 (http://www.who.int/wer/2010/wer8504.pdf), which correlates with more-severe disease in humans (1, 6, 13, 16, 32). However, these studies may overestimate the prevalence of viruses with the HA-222G mutation, since analysis has focused on severe cases. Moreover, viruses possessing Gly at this position have also been isolated from patients with mild symptoms. Nevertheless, these findings suggest that an amino acid characteristic for avian influenza viruses may increase virus pathogenicity in humans. Although the pathogenic potential of the HA-222G mutation has been tested in mouse and ferret models, the results were conflicting (8, 33). Here, therefore, we used a nonhuman primate model to evaluate the effect of HA-222G in two 2009 pandemic viruses isolated from patients who had severe clinical outcomes.

MATERIALS AND METHODS

Cells and viruses. Madin-Darby canine kidney (MDCK) cells were maintained in Eagle's minimal essential medium (MEM) containing 5% newborn calf serum. Human lung tissue samples were prepared and maintained as described previously (27).

A/Utah/42/09 and A/Wisconsin/WSLH26327/09 (2009 pandemic H1N1 influenza viruses), A/duck/Mongolia/301/01 (an avian H3N2 virus), and A/Tottori/45989/97 (a seasonal H3N2 virus) were used in this study. A/Utah/42/09 possessing HA-222G [Utah(HA222G)], a variant encoding HA-222D [Utah(HA222D)], A/Wisconsin/WSLH26327/09 possessing HA-222D [WSLH(HA222D)], and A/Wisconsin/WSLH26327/09 possessing HA-222G [WSLH(HA222G)] were generated by using reverse genetics (21) and completely sequenced to rule out unwanted mutations.

Plasmid construction. Reverse genetics systems were established by the method described by Neumann et al. (21). Briefly, viral cDNAs were synthesized by reverse transcription of viral RNAs (vRNAs) with oligonucleotide Uni-12 (5′-AGCAAAAGCAGG-3′) complementary to the conserved 3′ end of the vRNA, as previously described (12). The cDNAs were amplified by using PCR with gene-specific oligonucleotides and then inserted into the pHH21 vector.

The A/Utah/42/09 virus possesses glycine at position 222 in its HA protein. A pHH21 plasmid, encoding a variant HA with aspartic acid at this position, was generated by use of the QuikChange site-directed mutagenesis kit (Stratagene), according to the manufacturer's instructions.

Glycan array analyses. Viruses were grown in MDCK cells, clarified by low-speed centrifugation, laid over a cushion of 30% sucrose in phosphate-buffered saline (PBS), and ultracentrifuged at 25,000 rpm for 2 h at 4°C. Virus stocks were aliquoted and stored at −80°C. Virus concentrations were determined by use of a hemagglutination (HA) assay with 0.5% (vol/vol) turkey red blood cells. Custom microarray slides were printed for the CDC by using the CFG glycan library (CDC version 1 slides; see Table S1 in the supplemental material for the glycans) as described previously (4). Virus preparations were thawed and suspended in PBS supplemented with 3% (wt/vol) bovine serum albumin (BSA) to an HA titer of 128, established to be optimal for glycan array analyses. Virus suspensions were supplemented with 300 nM zanamivir, overlaid on the printed region of the slides, and then incubated with gentle agitation in a closed container for 1 h at room temperature. Unbound virus was then eluted with brief rinses in PBS. Slides were immediately incubated with hyperimmune sheep or ferret serum to A/California/07/09 (H1N1) HA (30 min), a biotinylated anti-sheep or ferret-IgG antibody (30 min), and a streptavidin-Alexa Fluor 635 conjugate (30 min) (Invitrogen, Carlsbad, CA) with brief PBS washes between incubations. After the final PBS wash, slides were briefly rinsed in deionized water, dried under a gentle stream of air, and immediately subjected to imaging. Fluorescence intensities were captured by using a ProScanArray HT (PerkinElmer, Waltham, MA). Image analyses were carried out with ImaGene 8 software (BioDiscovery, El Segundo, CA). Data were processed in MS Excel to group similar sialoglycans and generate a simplified chart.

Virus infection of human lung tissue. Fresh, surgically removed normal human lung specimens that contained alveoli were cut into ≈5-mm^3 cubes, washed with culture medium (F-12K nutrient mixture with 15% fetal calf serum [FCS], L-glutamine, and antibiotics), and incubated with virus (200 μl of a virus preparation containing 10^7 PFU/ml) at 37°C. Twelve hours postinfection, tissue blocks were fixed with 10% neutral buffered formalin and processed for routine paraffin embedding and immunofluorescence double staining or immunohistochemical analysis with a rabbit anti-influenza A virus antibody (R309, anti-H1N1; prepared in our laboratory) and mouse anti-surfactant protein A (PE10; Dako Japan Inc., Tokyo, Japan). Cells were incubated with Alexa-488-conjugated goat anti-rabbit IgG, Alexa-594-conjugated goat anti-mouse IgG, and DAPI (4′,6-diamidino-2-phenylindole). Samples were observed under a fluorescence microscope (BZ-8000; Keyence Co., Osaka, Japan). The infected tissue samples were also used for immunohistochemical analysis with a rabbit anti-influenza A virus antibody (R309), and the reactions were visualized by using a two-step dextran polymer system (Dako) and 3,3′-diamino benzidine (DAB). Human research ethics approval for use of all human specimens was obtained from the Kobe University Office of Research Ethics.

To assess the replication efficiency of viruses possessing HA-222G or HA-222D in human lung tissue, 5-mm^3 cubes of tissue were infected with 10^8 PFU/0.1 ml of concentrated virus and incubated for 1 h at 37°C in 5% CO_2. Tissues were washed with medium three times, and 600 μl of growth medium was then added. RNA samples were extracted from the culture supernatants collected from the infected tissues at 0, 24, 48, and 72 h postinfection and then subjected to real-time PCR to quantify the viral RNA encoding M1 protein.

Experimental infection of nonhuman primates. Two- to 4-year-old cynomolgus macaques, which were obtained from Harlan Laboratories (Madison, WI), Charles River Laboratories BRL (Houston, TX), and Shiga University of Medical Science (Shiga, Japan), who originally obtained the animals from Vietnam, were used according to approved protocols for the care and use of animals. As described elsewhere (10), animals were anesthetized with ketamine via intramuscular injection and inoculated with a suspension containing a total of 6.7×10^7 PFU of the respective virus through a combination of intratracheal (4.5 ml), intranasal (0.5 ml per nostril), ocular (0.1 ml per eye), and oral (1 ml) routes. Through implanted chips, macaques were monitored every day for changes in body temperature. On days 1, 3, 5, and 7 postinfection, nasal washes and bronchoalveolar lavage (BAL) samples were collected from animals. The BAL procedures were performed by first introducing a red rubber feeding tube into the tracheal lumen with the aid of a laryngoscope. Up to 3 ml of 1% lidocaine was instilled to control bronchospasm, as needed. The tip of the feeding tube was then gently wedged into a subsidiary bronchus, and lavage was performed by infusion of four 10-ml aliquots of sterile, pyrogen-free saline into the bronchus followed by aspiration using a 10-ml syringe. Typically, 25 to 35 ml of lavage fluid was recovered.

At the indicated time points postinfection, two or three macaques per group were euthanized for virologic and pathological examinations. The virus titers in various organs, nasal washes, and BAL fluid were determined by using plaque assays in MDCK cells.

Pathological examination. Tissues of animals were preserved in 10% phosphate-buffered formalin for pathological examination. They were then processed for routine paraffin embedding and cut into 5-μm-thick sections. One section from each tissue sample was subjected to standard hematoxylin-and-eosin staining, while another was processed for immunohistological staining with an anti-influenza virus rabbit antibody (R309) that reacts comparably with all of the test viruses. Specific antigen-antibody reactions were visualized by use of 3,3′-diaminobenzidine tetrahydrochloride staining and a Dako EnVision system (Dako Co. Ltd., Tokyo, Japan).

Cytokine and chemokine measurement. Cytokines and chemokines in the BAL fluid of macaques were measured by using the Milliplex MAP nonhuman

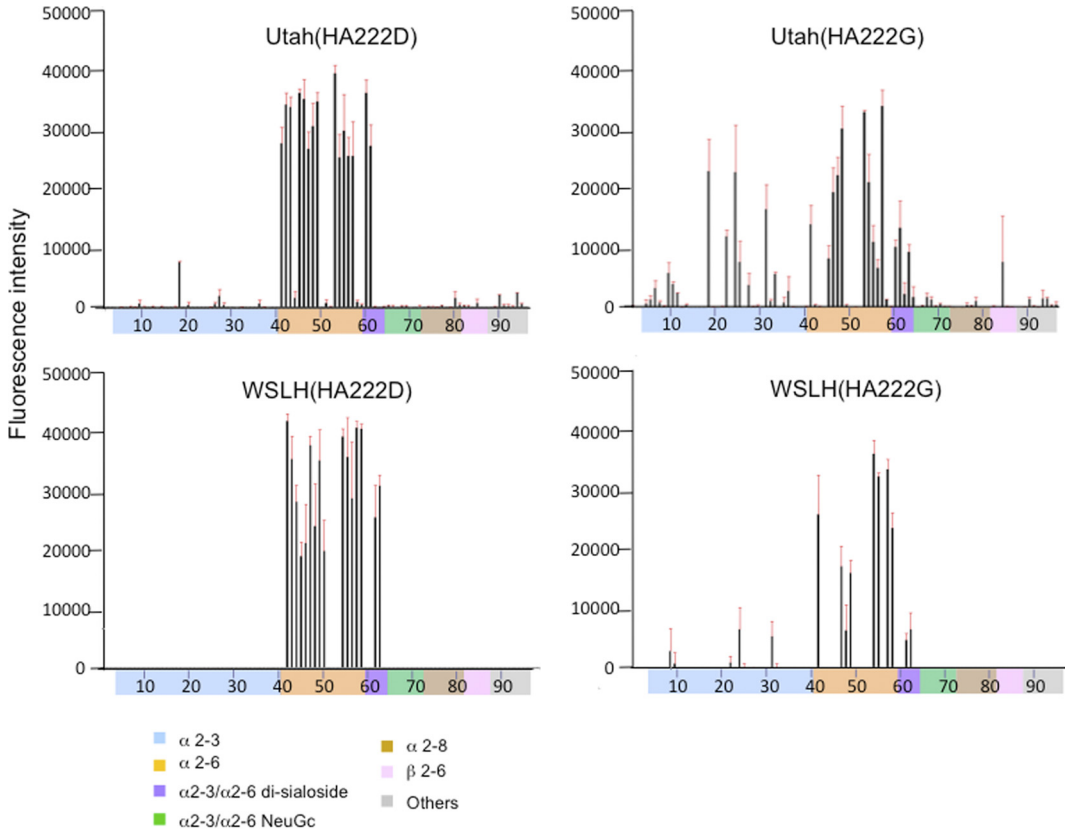

FIG. 1. Receptor specificity of 2009 pandemic H1N1 influenza viruses. Sialylated glycan binding by viruses possessing HA-222D or HA-222G; purified whole virions were analyzed by use of glycan microarrays. The microarrays displayed 86 sialylated and 9 asialo-glycans printed on coated glass slides. Different types of glycans on the array (*x* axis) are highlighted in different colors; the identity of each numbered glycan is provided in Table S1 in the supplemental material. The fluorescence signal for glycan #18 in the Utah virus pair includes nonspecific binding by the primary sheep antibody and cannot be interpreted as viral (data not shown). Such nonspecific binding was not observed with the WSLH virus pair, since we used a ferret primary antibody. Different types of terminal sialic-acid linkage to galactose of arrayed glycans are highlighted in different colors. Black bars denote the mean fluorescent binding signal intensity (*y* axis) of 4 spots; the standard error is shown as a red extension.

primate cytokine/chemokine panel (Millipore, Bedford, MA) with the Bio-Plex 200 system (Bio-Rad Laboratories, Hercules, CA).

RESULTS

Receptor specificity of 2009 pandemic H1N1 viruses that possess HA-222G. To evaluate the effect of HA-222G in 2009 pandemic viruses, we used two viruses, isolated from patients who had severe clinical outcomes, and their variants that differed only at position 222 in HA. One pair was derived from A/Utah/42/09 possessing HA-222G [Utah (HA222G)] and an artificially generated variant encoding HA-222D [Utah(HA222D)]. Another virus pair was derived from A/Wisconsin/WSLH26327/09, which was grown in MDCK cells or embryonated chicken eggs, resulting in the generation of variants possessing HA-222D [WSLH (HA222D)] or HA-222G [WSLH(HA222G)], respectively, while otherwise being identical. The original isolate likely contained both variants; however, propagation of H1N1 influenza viruses in MDCK cells or embryonated chicken eggs is known to select HA-222D or HA-222G variants, respectively (11, 25, 29). All test viruses were generated by using reverse genetics (21) and their genomes completely sequenced to rule out unwanted mutations.

Recent reports show that pandemic H1N1 viruses possessing a Gly residue at HA-222 bind to SAα2,3Gal as well as to SAα2,6Gal glycans, whereas viruses possessing HA-222D preferentially bind to only SAα2,6Gal glycans (8, 15, 34). In agreement with these reports, among the virus pairs we tested, viruses possessing HA-222G preferentially bound to SAα2,3Gal glycans compared to viruses with HA-222D (Fig. 1).

Infectivity of pandemic H1N1 viruses that possess HA-222G in human lung cells. Recent reports showed virus replication in the lung alveolar type II pneumocytes of a patient who died from pandemic H1N1 virus infection (20, 26); sequencing of virus directly derived from the lung of this patient revealed the HA-222G mutation (GISAID accession number EPI226248). Since human type II pneumocytes express SAα2,3Gal (27), 2009 pandemic H1N1 viruses that recognize avian-type receptors may efficiently infect these cells. To test this possibility, we incubated surgically excised human alveolar lung tissue with 2×10^6 PFU of virus and assessed viral antigen expression 12 h later. This time point was chosen because virus-infected alveolar cells were lost at 18 h postinfection, likely due to cytopathic effects. As shown in Fig. 2A, for viruses possessing HA-222G [i.e., Utah(HA222G), WSLH(HA222G), and avian

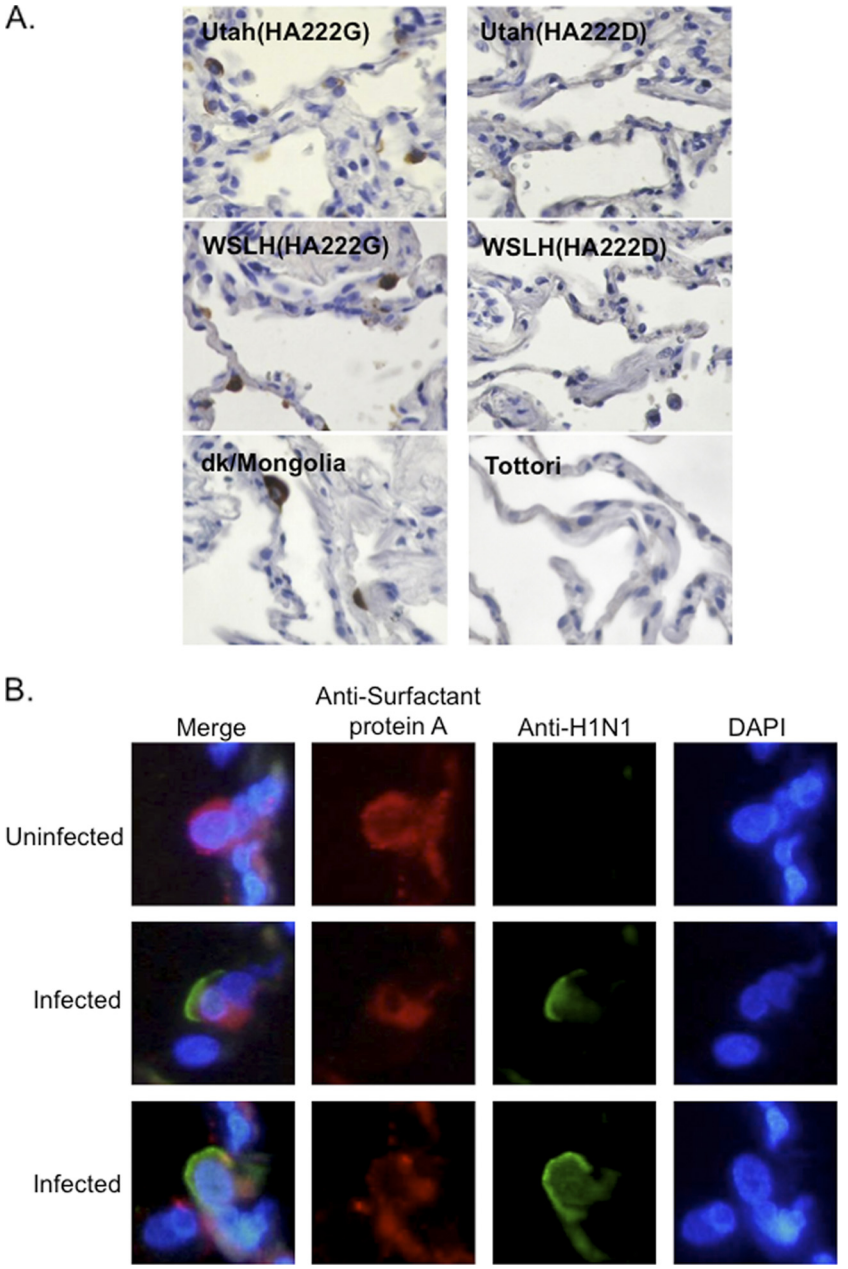

FIG. 2. Infection of human lung tissue with 2009 pandemic H1N1 viruses possessing HA-222G or HA-222D. (A) For the control avian virus (A/duck/Mongolia/301/01; dk/Mongolia), as well as Utah(HA222G) and WSLH(HA222G) viruses, viral antigen (brown stain) was detected in type II pneumocytes, whereas viral antigen-positive cells were not detected with Utah(HA222D), WSLH(HA222D), or a seasonal H3N2 virus A/Tottori/45989/97 (Tottori). (B) Human lung tissue was incubated with Utah(HA222G) virus (200 μl of a virus preparation containing 10^7 PFU/ml). Viral antigen (green) and type II pneumocytes (red), which express surfactant protein A, were detected in the tissue. The nucleus is stained with DAPI (blue). Panels labeled as uninfected or infected indicate uninfected or infected pneumocytes, respectively. There were 596 and 1,203 virus antigen-positive cells detected in a total of 18 sections per lung tissue block (≈0.5-cm^3 cube) infected with Utah(HA222G) and WSLH(HA222G), respectively, whereas no positive cells were detected from lung tissues infected with the HA-222D-encoding counterparts of these viruses.

virus A/duck/Mongolia/301/01], viral antigens were detected in type II pneumocytes, which express surfactant protein A (Fig. 2B), at 12 h postinfection. By contrast, virus antigen-positive cells were not detected in lung tissues infected with viruses encoding HA-222D [i.e., Utah(HA222D), WSLH(HA222D), and seasonal H3N2 virus A/Tottori/45989/97] (Fig. 2A), as previously demonstrated with a seasonal H1N1 virus (27). Thus, efficient infection of type II pneumocytes in humans correlates with the ability to recognize avian-type receptors.

We further compared the growth properties of viruses possessing HA-222D or HA-222G in human lung tissue. We found that Utah(HA222G) and WSLH(HA222G) grew to higher titers than Utah(HA222D) and WSLH(HA222D), respectively (Fig. 3), suggesting that binding to SAα2,3Gal receptors may

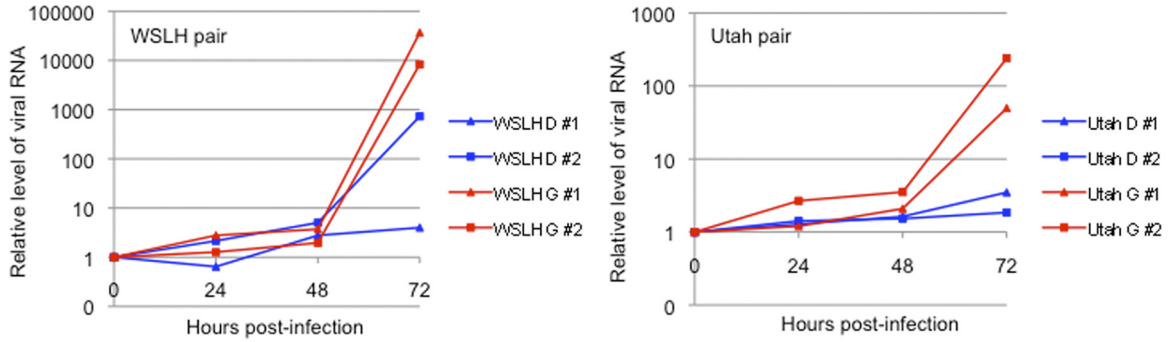

FIG. 3. Viral growth kinetics in human lung tissue. Human lung tissue was infected with 10^8 PFU/0.1 ml of Utah and WSLH virus pairs possessing HA-222G or HA-222D. RNA samples were extracted from the culture supernatants collected from the infected tissue at the indicated time points and then subjected to real-time-PCR to quantify viral RNA.

result in more-efficient infection. In addition, the viral RNA level in human lungs infected with WSLH(HA222G) was much higher than that in lungs infected with Utah(HA222G), consistent with the data in Fig. 2; that is, the number of viral antigen-positive cells in lungs infected with WSLH(HA222G) was higher than that in lungs infected with Utah(HA222G) (i.e., 1,203 versus 596 antigen-positive cells, respectively).

Pathogenicity of viruses that possess HA-222G in nonhuman primates. As described above, although a potential role for HA-222G in the pathogenicity of 2009 pandemic influenza viruses has been evaluated in mouse and ferret models, the results were conflicting (8, 33). Nonhuman primates are increasingly used as a model to assess highly pathogenic influenza virus infections because of their close genetic relationship to humans (2, 14, 23). We infected cynomolgus macaques (*Macaca fascicularis*) with 6.7×10^7 PFU of the Utah and WSLH virus pairs. Viruses were recovered from the upper respiratory tracts of animals infected with viruses possessing HA-222D more frequently than from their counterparts encoding HA-222G (as demonstrated by the virus detection frequency in nasal washes) (Table 1); this finding is consistent with a recent report of a virus possessing HA-222D found mainly in the upper respiratory tract of pigs (5). By contrast, infection with viruses possessing HA-222G or HA-222D resulted in similar titers in the lower respiratory tract on days 1, 3, and 5 postinfection. The Utah(HA222G) virus, but not Utah(HA222D), was also recovered from the BAL fluid of one animal on day 7 postinfection (Table 1). Further, two or three animals per group were euthanized for virologic and pathological analyses at the indicated times after infection. There were no appreciable differences in virus replication between Utah(HA222D)- and Utah(HA222G)-infected animals (Table 2); however, macroscopic pathological changes, such as severe hyperemia, congestion, and red hepatization were observed in larger areas of the lungs of animals infected with Utah(HA222G) (Fig. 4A2) than in those of Utah(HA222D)-infected animals (Fig. 4A1). Histologically, pulmonary edema was observed more widely in the lungs of animals infected with Utah(HA222G) virus [two-thirds of the examined lung lobes of the Utah(HA222G)-infected animals contained edematous lesions [Fig. 4A5 and A8]) compared to the lungs of animals infected with Utah(HA222D) (less than one-quarter of the examined lobes were edematous [Fig. 4A4 and A7]). In addition, the number of virus antigen-positive regenerative hyperplastic type II pneumocytes (Fig. 4A11 white arrowheads) was substantially higher in the lungs of animals infected with Utah(HA222G) than in those infected with Utah(HA222D) (Fig. 4A10). These findings demonstrate that infection with Utah(HA222G) causes alveolar damage more severe than that with Utah(HA222D). These pathological differences were not observed for the WSLH virus pair (Fig. 4B).

We also investigated whether the differences in pathogenesis

TABLE 1. Virus titers in respiratory washes from infected cynomolgus macaques[a]

Sample	Day	Virus titer ($\log_{10}$ PFU/ml) of indicated animal infected with[b]:											
		Utah(HA222D)			Utah(HA222G)			WSLH(HA222D)			WSLH(HA222G)		
		#392	#393	#394	#395	#396	#397	#401	#402	#403	#398	#399	#400
Nasal wash	1	2.6	—	2.6	—	—	—	—	2.1	—	—	2.0	—
	3	—	—	—	—	—	—	1.6	—	1.9	1.8	—	—
	5	2.0	—	—	2.0	—	—	—	—	—	—	1.6	—
	7	2.5	—	1.5	—	—	—	—	2.0	2.7	—	—	—
BAL fluid	1	5.8	5.7	6.0	4.9	6.0	5.4	3.4	4.4	5.0	3.9	5.3	5.3
	3	5.3	4.7	5.0	4.4	3.8	4.8	3.0	4.7	4.0	3.4	2.9	4.2
	5	4.0	5.4	4.3	4.1	4.2	4.6	3.8	5.2	3.3	5.5	5.2	3.4
	7	—	—	—	3.0	—	—	—	—	—	—	—	—

[a] Cynomolgus macaques were infected with 6.7×10^7 PFU of virus (6.7 ml) via multiple routes. Nasal washes and BAL samples were collected every other day for virus titration.

[b] —, virus not detected (detection limit, 1.3 $\log_{10}$ PFU/ml). Numbers (#392 to #403) are animal IDs.

TABLE 2. Virus titers in organs of infected cynomolgus macaques[a]

Organ	Virus titer (log_{10} PFU/g) of indicated animal infected with[b]:									
	Utah(HA222D)					Utah(HA222G)				
	Day 3 pi		Day 6 pi			Day 3 pi		Day 6 pi		
	#1	#2	#3	#4	#5	#7	#8	#9	#10	#11
Tonsil	4.9	—	—	—	—	5.1	2.8	—	—	—
Trachea	4.3	5.1	—	—	—	5.6	3.7	—	—	—
Bronchus (right)	3.7	5.3	—	—	—	3.0	4.4	—	—	—
Bronchus (left)	—	4.3	—	—	—	4.0	3.6	—	—	—
Lung (upper right)	6.5	2.8	—	—	—	—	5.3	—	—	—
Lung (middle right)	3.1	2.5	—	—	—	4.4	4.7	—	—	—
Lung (lower right)	6.5	—	4.1	4.4	—	3.9	5.5	—	—	—
Lung (upper left)	3.7	—	—	—	—	—	3.9	—	—	—
Lung (middle left)	3.8	NA	—	—	—	—	7.5	—	—	4.0
Lung (lower left)	4.3	4.1	—	—	3.7	5.3	7.2	—	4.7	—

[a] Cynomolgus macaques were inoculated with 6.7×10^7 PFU of virus through multiple routes. Two or three macaques per group were sacrificed on days 3 or 6 postinfection (pi) for virus titration, respectively.

[b] —, virus not detected (detection limit: 1.3 log_{10} PFU/g). Numbers (#1 to #11) are animal IDs.

of Utah(HA222D) and Utah(HA222G) were associated with altered host responses to infection by measuring cytokine and chemokine levels in the BAL fluid of infected monkeys. On day 1 postinfection, proinflammatory cytokines and chemokines (i.e., macrophage inflammatory protein-1 [MCP-1], MIP-1β, MIP-1α, interleukin-1β [IL-1β], IL-6, tumor necrosis factor alpha [TNF-α], granulocyte-macrophage colony-stimulating factor [GM-CSF], and G-CSF) were detected in the BAL fluid of most of the infected animals (Fig. 5). The magnitudes of cytokine/chemokine induction appeared comparable among all animals, with one exception: a Utah(HA222G)-infected animal (ID 396) with a high virus titer and high cytokine/chemokine levels relative to those of the other animals (Table 1 and Fig. 5). On day 7 postinfection, the IL-1 receptor α (IL-1Rα) levels were high in two of three animals infected with Utah(HA222D) virus (Fig. 5A), implying that tissue repair and remodeling of the alveolar architecture followed viral clearance but that this may be delayed in Utah(HA222G)-infected animals (19, 22). Taken together, these results suggest that there is no appreciable correlation between the level of proinflammatory cytokines/chemokines and the severity of lung pathology.

DISCUSSION

Here, we demonstrated that the Asp-to-Gly change at position 222 of HA increases binding to avian-type receptors and that infection with a 2009 pandemic H1N1 virus possessing HA-222G [i.e., Utah(HA222G) virus], which resulted in enhanced SAα2-3Gal binding, caused an increase in pathogenicity in the lungs of infected animals. Although we did not find a difference in virus titers in lung homogenates between viruses possessing HA-222G and HA-222D, this method does not allow the identification of specific cell types infected by the viruses. However, we showed that viruses with HA-222G infected type II pneumocytes of infected animals efficiently, as demonstrated in human lung tissue (Fig. 2A). We previously showed that a seasonal H1N1 virus (A/Kawasaki/UTK-4/2009), which infected a limited number of type I, but not type II, pneumocytes, caused less damage in the lungs of the virus-infected monkeys (10). Since type II pneumocytes produce pulmonary surfactant and differentiate to type I pneumocytes, which are critical for gas exchange in the alveoli (31), the preferential infection of this cell type by influenza virus may result in more-severe lung damage. Moreover, we found that much of the area surrounding the damaged alveoli in Utah(HA222G)-infected animals contained extensive regenerative hyperplastic type II pneumocytes that express SAα2,3Gal glycans (data not shown). Therefore, it is plausible that SAα2,3Gal-recognizing viruses possessing HA222-G target type II pneumocytes and newly regenerated type II pneumocytes, reducing the availability of progenitor cells for essential lung functions, thus causing severe pulmonary impairment, diffuse alveolar damage, and respiratory distress. Similar pathogenesis may apply to highly pathogenic avian influenza virus infection in humans (9, 27, 30).

Our glycan microarray revealed efficient binding of viruses with HA-222D to SAα2,6Gal glycans (Fig. 1), as expected for human influenza viruses. These viruses bound to most of the α2-6-sialylated glycans on the array, including branched, biantennary, and linear structures (but not the shortest glycans). Childs et al. (7) and Liu et al. (15) reported that 2009 pandemic H1N1 viruses also bind to some SAα2,3Gal glycans. However, Utah(HA222D) and WSLH(HA222D) (representing the 2009 pandemic H1N1 viruses) did not show any appreciable binding to SAα2,3Gal glycans (Fig. 1), which may be explained by the differences in the glycan array platforms used by us and them (7, 15). Briefly, our glycan microarray uses amine-reactive *N*-hydroxysuccinimide (NHS)-activated glass slides, which allow rapid covalent coupling of amine-functionalized glycans or glycoconjugates. For our analysis, we used purified virion suspended to an HA titer of 128, which was established as optimal for glycan array analyses. By contrast, in the previous two reports (7, 15), they used nitrocellulose-coated glass slides printed with lipid-linked oligosaccharide probes, and the viruses were analyzed at HA titers of 2,000, which is almost 15-fold higher than in our analyses. Therefore, we speculate that the differences in the conditions for the glycan array analyses likely caused the discrepancy between our results and those of the previous reports (7, 15).

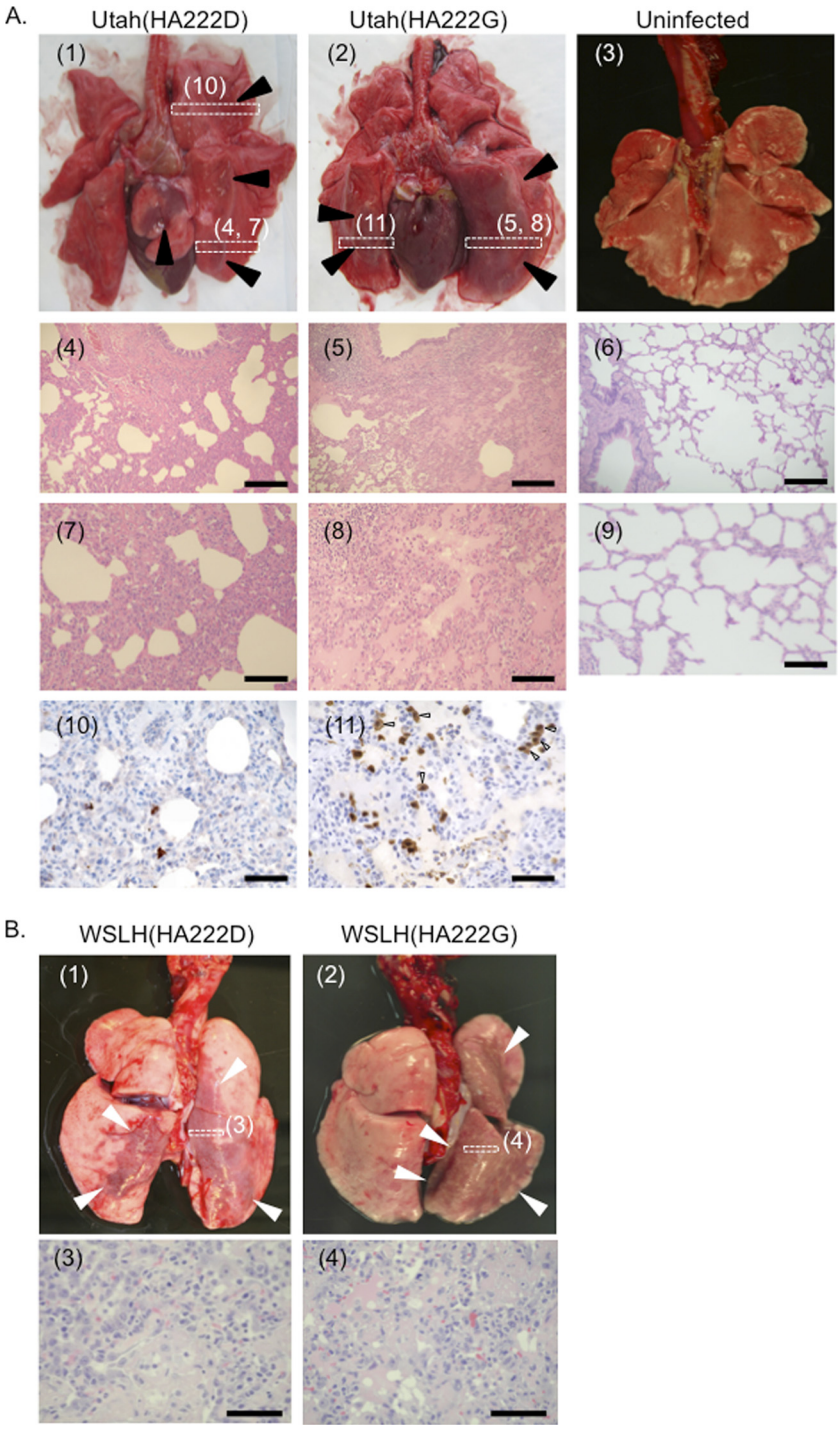

FIG. 4. Virus pathogenicity in nonhuman primates. (A) Macroscopic pathological changes were observed in a larger proportion of the lungs of animals infected with Utah(HA222G) (2) compared to those infected with Utah(HA222D) (1) on day 6 postinfection. Infection with Utah(HA222D) mainly resulted in bronchopneumonia with thickening of the alveolar walls (4). Higher magnification of the alveolar area shows severe thickening of the alveolar wall by infiltration of inflammatory cells (7); however, air-containing clear alveolar spaces and thin alveolar walls were observed in large areas of the lobes. By contrast, infection with Utah(HA222G) mainly resulted in severe pneumonia with prominent pulmonary edema and inflammatory infiltration (5). Higher magnification of the alveolar area revealed alveolar spaces filled with proteinaceous fluid and severe alveolitis (8). Numerous viral antigen-positive cells were detected in animals infected with Utah(HA222G) (11) compared to those infected with Utah(HA222D) (10). Lungs derived from an uninfected animal showed no gross or histological changes (3, 6, and 9). Black arrowheads indicate gross lesions in the lungs of infected animals. The boxes indicated by dotted lines depict the areas shown in the microscopic photos (1, 2). White arrowheads show large regenerative type II pneumocytes infected with Utah(HA222G) virus (11). Bars = 200 μm (4 to 6), 100 μm (7 to 9), 50 μm (10 and 11). (B) Lungs of macaques infected with WSLH(HA222D) (1 and 3) or WSLH(HA222G) (2 and 4) on day 7 postinfection. Arrowheads: gross lesions. The boxes depicted in dotted lines outline the areas shown in the microscopic photos. Bars = 50 μm.

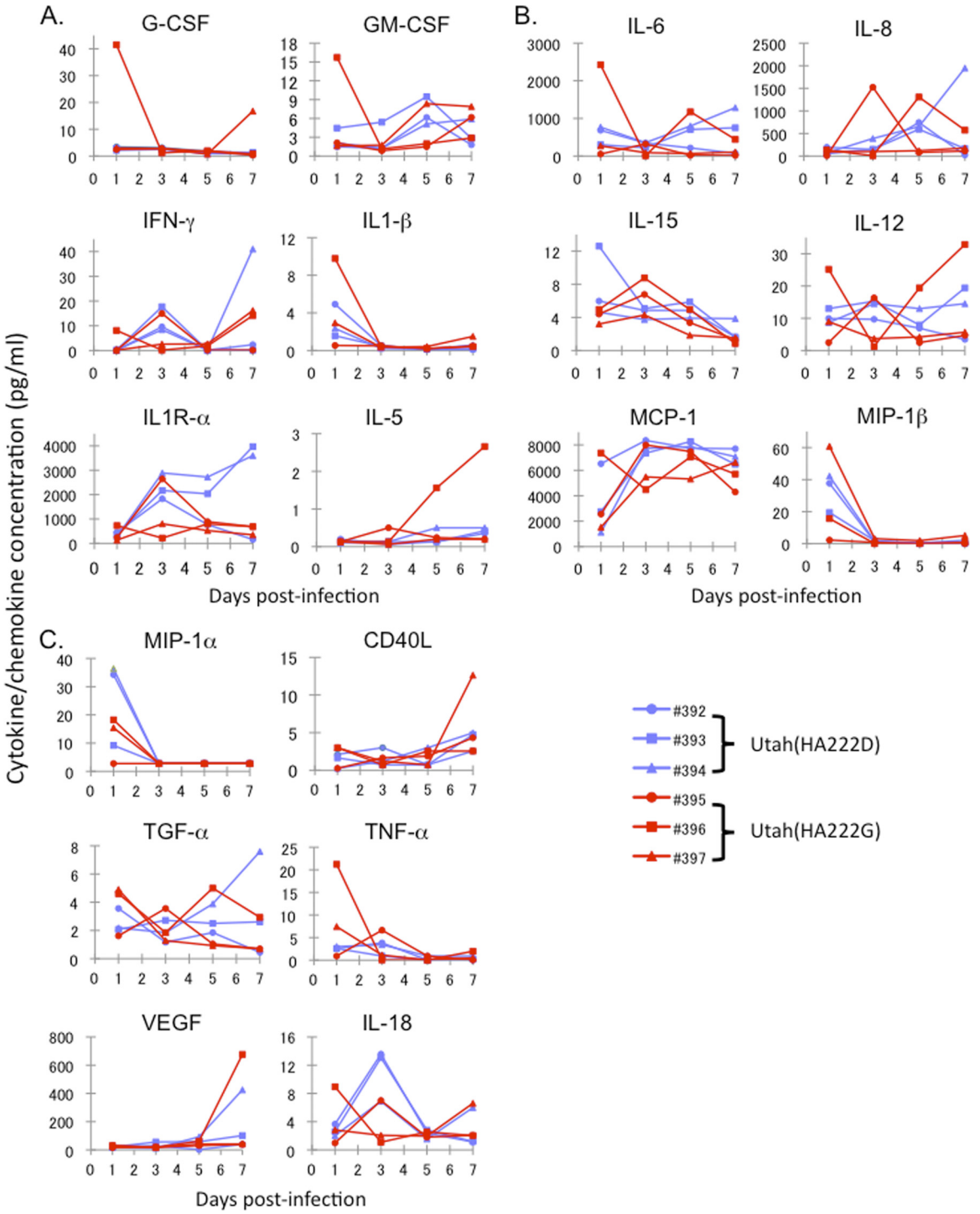

FIG. 5. Proinflammatory cytokine and chemokine responses in the lungs of infected cynomolgus macaques. Cytokines and chemokines were measured as described in Materials and Methods. The concentrations of various cytokines and chemokines in the BAL fluid of infected cynomolgus macaques were measured on days 1, 3, 5, and 7 postinfection by use of protein array analysis with the Milliplex MAP nonhuman primate cytokine/chemokine panel-premixed 23-Plex (Millipore, Bedford, MA). (A) G-CSF, GM-CSF, IFN-γ, IL-1β, IL1R-α, IL-5; (B) IL-6, IL-8, IL-15, IL-12, MCP-1, MIP-1β; and (C) MIP-1α, CD40L, transforming growth factor α (TGF-α), TNF-α, vascular endothelial growth factor (VEGF), and IL-18.

Recently, Chutinimitkul et al. (8) evaluated the role of HA-222G in pathogenicity and found no correlation between HA-222G and increased pathogenicity in mice and ferrets; by contrast, Xu et al. (33) reported enhanced pathogenicity in mice for this mutant. The discrepancy between the findings of Chutinimitkul et al. (8) and ours may originate from differences in the virus stains used. Chutinimitkul et al. (8) tested A/Netherlands/602/2009, which was isolated from a mild case very early

in the 2009 pandemic (29 April 2009), whereas we tested A/Utah/42/2009, which was isolated from a severe case later in the pandemic (24 July 2009). When we tested A/Wisconsin/WSLH26327/2009, which was isolated from a severe case early in the pandemic (5 May 2009 or earlier), the HA-222G substitution had no effect on the lung pathology of the infected animals (Fig. 4B). Since there are many amino acid differences between A/Netherlands/602/2009, A/Wisconsin/WSLH26327/2009, and A/Utah/42/2009 (see Table S2 in the supplemental material), the combination of HA-222G with other amino acid changes in other viral proteins may influence changes in pathogenicity in mammals. In addition, the different animal models used in these studies may have contributed to the different outcomes. We should also consider the possible contribution of host genetics to the consequences of influenza virus infection (i.e., mild or severe disease outcome). Taken together, the HA-222G substitution appears to increase the pathogenicity of influenza viruses in mammals under certain conditions and, as such, could be considered a virulence maker.

ACKNOWLEDGMENTS

We thank Li-Mei Chen and Ruben Donis for receptor-binding analyses. We also thank Jasmyni Dias, Kerry Beheler, Carissa Boettcher, Nichole Goecks, Jennifer Post, Martha McGregor, Kelly Moore, Ashley Luka, Hiromi Sakawaki, Yuko Sakai-Tagawa, Naomi Fujimoto, Kazue Goto, and Asako Nakagawa for technical support. We thank Susan Watson and Krisna Wells for editing the manuscript.

The glycan microarray was produced for the Centers for Disease Control and Prevention (CDC) by using a glycan library generously provided by the Consortium for Functional Glycomics funded by National Institute of General Medical Sciences grant GM62116. This work was supported by National Institute of Allergy and Infectious Diseases, Public Health Service research grants; by an NIAID-funded Center for Research on Influenza Pathogenesis (CRIP, HHSN266200700010C); by Grant-in-Aid for Specially Promoted Research; by a contract research fund for the Program of Founding Research Centers for Emerging and Reemerging Infectious Diseases from the Ministry of Education, Culture, Sports, Science, and Technology; by grants-in-aid from the Ministry of Health; and by ERATO (Japan Science and Technology Agency). This work was also supported by NIH National Center for Research Resources grant P51 RR000167 to the Wisconsin National Primate Research Center, by a National Heart, Lung and Blood Institute research grant (1U01AI082982), and by a U.S. Army Medical Research and Material Command research grant (W81XWH-07-1-0550).

REFERENCES

1. **Anton, A., et al.** 2010. D225G mutation in the hemagglutinin protein found in 3 severe cases of 2009 pandemic influenza A (H1N1) in Spain. Diagn. Microbiol. Infect. Dis. **67:**207–208.
2. **Baskin, C. R., et al.** 2009. Early and sustained innate immune response defines pathology and death in nonhuman primates infected by highly pathogenic influenza virus. Proc. Natl. Acad. Sci. U. S. A. **106:**3455–3460.
3. **Bautista, E., et al.** 2010. Clinical aspects of pandemic 2009 influenza A (H1N1) virus infection. N. Engl. J. Med. **362:**1708–1719.
4. **Blixt, O., et al.** 2004. Printed covalent glycan array for ligand profiling of diverse glycan binding proteins. Proc. Natl. Acad. Sci. U. S. A. **101:**17033–17038.
5. **Brookes, S. M., et al.** 2010. Replication, pathogenesis and transmission of pandemic (H1N1) 2009 virus in non-immune pigs. PLoS One **5:**e9068.
6. **Chen, H., et al.** 2010. Quasispecies of the D225G Substitution in the Hemagglutinin of Pandemic Influenza A(H1N1) 2009 Virus from Patients with Severe Disease in Hong Kong, China. J. Infect. Dis. **201:**1517–1521.
7. **Childs, R. A., et al.** 2009. Receptor-binding specificity of pandemic influenza A (H1N1) 2009 virus determined by carbohydrate microarray. Nat. Biotechnol. **27:**797–799.
8. **Chutinimitkul, S., et al.** 2010. Virulence-associated substitution D222G in the hemagglutinin of 2009 pandemic influenza A(H1N1) virus affects receptor binding. J. Virol. **84:**11802–11813.
9. **Guarner, J., and R. Falcon-Escobedo.** 2009. Comparison of the pathology caused by H1N1, H5N1, and H3N2 influenza viruses. Arch. Med. Res. **40:**655–661.
10. **Itoh, Y., et al.** 2009. In vitro and in vivo characterization of new swine-origin H1N1 influenza viruses. Nature **460:**1021–1025.
11. **Katz, J. M., C. W. Naeve, and R. G. Webster.** 1987. Host cell-mediated variation in H3N2 influenza viruses. Virology **156:**386–395.
12. **Katz, J. M., M. Wang, and R. G. Webster.** 1990. Direct sequencing of the HA gene of influenza (H3N2) virus in original clinical samples reveals sequence identity with mammalian cell-grown virus. J. Virol. **64:**1808–1811.
13. **Kilander, A., R. Rykkvin, S. G. Dudman, and O. Hungnes.** 2010. Observed association between the HA1 mutation D222G in the 2009 pandemic influenza A(H1N1) virus and severe clinical outcome, Norway 2009–2010. Euro Surveill. **15:**Article 2.
14. **Kobasa, D., et al.** 2007. Aberrant innate immune response in lethal infection of macaques with the 1918 influenza virus. Nature **445:**319–323.
15. **Liu, Y., et al.** 2010. Altered receptor specificity and cell tropism of D222G haemagglutinin mutants from fatal cases of pandemic A(H1N1) 2009 influenza. J. Virol. **84:**12069–12074.
16. **Mak, G. C., et al.** 2010. Association of D222G substitution in haemagglutinin of 2009 pandemic influenza A (H1N1) with severe disease. Euro Surveill. **15:**Article 4.
17. **Matrosovich, M., et al.** 2000. Early alterations of the receptor-binding properties of H1, H2, and H3 avian influenza virus hemagglutinins after their introduction into mammals. J. Virol. **74:**8502–8512.
18. **Matrosovich, M. N., A. S. Gambaryan, and H.-D. Klenk.** 2008. Receptor specificity of influenza viruses and its alteration during interspecies transmission, p. 134–155. *In* H.-D. Klenk, M. N. Matrosovich, and J. Stech (ed.), Avian influenza, vol. 27. Karger, Basel, Switzerland.
19. **Mura, M., C. C. dos Santos, D. Stewart, and M. Liu.** 2004. Vascular endothelial growth factor and related molecules in acute lung injury. J. Appl. Physiol. **97:**1605–1617.
20. **Nakajima, N., et al.** 2010. The first autopsy case of pandemic influenza (A/H1N1pdm) virus infection in Japan: detection of a high copy number of the virus in type II alveolar epithelial cells by pathological and virological examination. Jpn. J. Infect. Dis. **63:**67–71.
21. **Neumann, G., et al.** 1999. Generation of influenza A viruses entirely from cloned cDNAs. Proc. Natl. Acad. Sci. U. S. A. **96:**9345–9350.
22. **Park, J. W., et al.** 2004. Interleukin-1 receptor antagonist attenuates airway hyperresponsiveness following exposure to ozone. Am. J. Respir. Cell Mol. Biol. **30:**830–836.
23. **Rimmelzwaan, G. F., et al.** 2001. Pathogenesis of influenza A (H5N1) virus infection in a primate model. J. Virol. **75:**6687–6691.
24. **Rogers, G. N., T. J. Pritchett, J. L. Lane, and J. C. Paulson.** 1983. Differential sensitivity of human, avian, and equine influenza A viruses to a glycoprotein inhibitor of infection: selection of receptor specific variants. Virology **131:**394–408.
25. **Schild, G. C., J. S. Oxford, J. C. de Jong, and R. G. Webster.** 1983. Evidence for host-cell selection of influenza virus antigenic variants. Nature **303:**706–709.
26. **Shieh, W. J., et al.** 2010. 2009 pandemic influenza A (H1N1): pathology and pathogenesis of 100 fatal cases in the United States. Am. J. Pathol. **177:**166–175.
27. **Shinya, K., et al.** 2006. Avian flu: influenza virus receptors in the human airway. Nature **440:**435–436.
28. **Stevens, J., et al.** 2006. Glycan microarray analysis of the hemagglutinins from modern and pandemic influenza viruses reveals different receptor specificities. J. Mol. Biol. **355:**1143–1155.
29. **Takemae, N., et al.** 2010. Alterations in receptor-binding properties of swine influenza viruses of the H1 subtype after isolation in embryonated chicken eggs. J. Gen. Virol. **91:**938–948.
30. **van Riel, D., et al.** 2006. H5N1 virus attachment to lower respiratory tract. Science **312:**399.
31. **Williams, M. C.** 2003. Alveolar type I cells: molecular phenotype and development. Annu. Rev. Physiol. **65:**669–695.
32. **World Health Organization.** 2009. Public health significance of virus mutation detected in Norway. World Health Organization, Geneva, Switzerland.
33. **Xu, L., et al.** 2010. A single-amino-acid substitution in the HA protein changes the replication and pathogenicity of the 2009 pandemic A (H1N1) influenza viruses in vitro and in vivo. Virol. J. **7:**325.
34. **Yang, H., P. Carney, and J. Stevens.** 2010. Structure and receptor binding properties of a pandemic H1N1 virus hemagglutinin. PLoS Curr. **2:**RRN1152.